

Seasonality in precipitation variability over Europe

Igor I. Zveryaev

P. P. Shirshov Institute of Oceanology, Moscow, Russia

Received 7 April 2003; revised 30 December 2003; accepted 22 January 2004; published 6 March 2004.

[1] A gridded monthly and pentad precipitation for 1979–2001 from the Climate Prediction Center Merged Analysis of Precipitation (CMAP) data set and terrestrial monthly gauge-based precipitation for 1958–1998 from the Climatic Research Unit, University of East Anglia (CRU), data set are used to investigate seasonality in the long- and short-term precipitation variability over Europe. Prominent seasonal differences are detected both in precipitation climatologies and in characteristics of precipitation variability. It is shown that over western Europe the summer precipitation climatology and its year-to-year variability (expressed by standard deviations) are lower than those of the winter precipitation. Major seasonal differences are found over central eastern Europe. In this region the summer precipitation climatology and magnitudes of its interannual variability exceed respective winter characteristics by a factor of 2–3.5. Similar relationships are found for the summer and winter magnitudes of intraseasonal fluctuations of precipitation. The first empirical orthogonal function (EOF) modes of both summer and winter seasonal mean precipitation over Europe are associated with the North Atlantic Oscillation (NAO). However, they explain very different (42% for winter and 25% for summer) fractions of total precipitation variability and form principally different spatial patterns. Temporal behavior of the respective principal components is also essentially different. The first EOF mode of the winter magnitudes of intraseasonal precipitation fluctuations is also associated with the NAO. The second EOF mode of the winter precipitation is linked to the East Atlantic teleconnection pattern. However, the respective mode in the magnitudes of intraseasonal fluctuations was not detected. The second EOF mode of the summer precipitation is associated with the 500 hPa heights pattern, which is characterized by four anomaly centers. Two major centers of opposite polarity are located over western Europe and Scandinavia-northeastern European Russia. INDEX

TERMS: 1620 Global Change: Climate dynamics (3309); 1854 Hydrology: Precipitation (3354); 3309

Meteorology and Atmospheric Dynamics: Climatology (1620); 3319 Meteorology and Atmospheric

Dynamics: General circulation; 9335 Information Related to Geographic Region: Europe; KEYWORDS: precipitation, teleconnections, Europe

Citation: Zveryaev, I. I. (2004), Seasonality in precipitation variability over Europe, *J. Geophys. Res.*, 109, D05103, doi:10.1029/2003JD003668.

1. Introduction

[2] Changes in precipitation over Europe are of serious consequence to a wide range of human activities in this densely populated region. Precipitation variability at the different timescales directly affects many European economies. For example, during summer 2002, extremely dry conditions in central European Russia resulted in extensive forest fires in the region, while anomalously high precipitation caused floods in central eastern Europe and the southern part of European Russia. On the other hand, in July to early August of 2003 almost all of western central Europe suffered from deficient precipitation and extremely high temperatures that caused, in particular, catastrophic forest fires in southern France, Spain, and Portugal. Thus

both deficient and excessive precipitation resulted in significant damage to the regional economies.

[3] The relationship between different climatic variables (e.g., air temperature, precipitation, etc.) in the Atlantic-European sector and the atmospheric circulation has been the subject of many observational and modeling studies in the past. Most of these studies were focused on the cold season [Hurrell, 1995; Wibig, 1999; Rodwell *et al.*, 1999; Zveryaev, 1999; Cassou and Terray, 2001; Drevillon *et al.*, 2001]. Such interest in the winter climate is understandable, because winter months are dynamically the most active, and therefore perturbations in the atmospheric circulation can grow to large amplitudes. Less attention has been given in past years to the seasonality [Shabalova and Weber, 1998; Portis *et al.*, 2001; Slonosky *et al.*, 2001] of climate variations in the Atlantic-European sector, and, in particular, to summer climate variability [Colman and Davey, 1999; Hurrell and Folland, 2002]. However, sum-

mer precipitation over most of central eastern Europe and Scandinavia is essentially greater than that during the winter. Figure 1e shows that over a large portion of Europe summer precipitation exceeds that of winter by an order of 2 or more. In comparison with winter precipitation, interannual variability (expressed as standard deviations of seasonal means) of summer precipitation is also essentially higher over most of eastern Europe and Scandinavia (Figure 1f). It is thus useful to study further the seasonality of the precipitation variability over Europe at the different timescales.

[4] Because of the known problems in prediction of boreal summer climate in midlatitudes [Johansson *et al.*, 1998; Colman and Davey, 1999; Dirmeyer *et al.*, 2003], further detailed analysis of the variability of summer climate is extremely important. Although observational data analysis alone may not be able to disclose the cause-and-effect relationship between different components of the summer climate system, understanding the observational links may lead to an improved ability for seasonal predictions of the European climate.

[5] During the past 2 decades, analysis of spatial-temporal variability of the precipitation has received considerable attention. A number of authors focused on the regional changes in precipitation [Zorita *et al.*, 1992; von Storch *et al.*, 1993; Hurrell, 1995; Wibig, 1999; Corte-Real *et al.*, 1998; Qian *et al.*, 2000]. Several others considered global distribution of precipitation and its variability [Bradley *et al.*, 1987; Diaz *et al.*, 1989; Dai *et al.*, 1997; Dai and Wigley, 2000]. Most of the aforementioned studies are based on analysis of the winter or annual mean precipitation. Less emphasis, however, has been placed on the analysis of spatial-temporal variability of the summer precipitation.

[6] The present study focuses on the analysis of the summer and winter precipitation variability at different timescales and on the possible links between this variability and major teleconnection patterns of the atmospheric circulation. The study is aimed at the detection of the leading modes of seasonal mean summer and winter precipitation and of the magnitudes of intraseasonal precipitation fluctuations during the two seasons. Another objective is establishing the associations between the aforementioned modes of precipitation variability and teleconnection patterns that characterize atmospheric circulation in the region. The primary concern is to identify the prominent seasonal differences in precipitation variability over Europe.

[7] In the present study we analyze long- and short-term variability of precipitation over Europe on the basis of relatively continuous in time and spatially homogeneous data of precipitation available from the Climate Prediction Center Merged Analysis of Precipitation (CMAP) [Xie and Arkin, 1996, 1997] and from the Climatic Research Unit, University of East Anglia (CRU) [New *et al.*, 1999, 2000], data sets. Special emphasis is made on the seasonal differences in precipitation variability. The data used and analysis methods are described in section 2. Seasonal climatologies and interannual variability of precipitation during 1979–2001 are considered in section 3. Intraseasonal variability of precipitation is analyzed in section 4. Links between leading modes of precipitation variability and major teleconnection

patterns are examined in section 5. Finally, a summary and discussion are presented in section 6.

2. Data and Methods

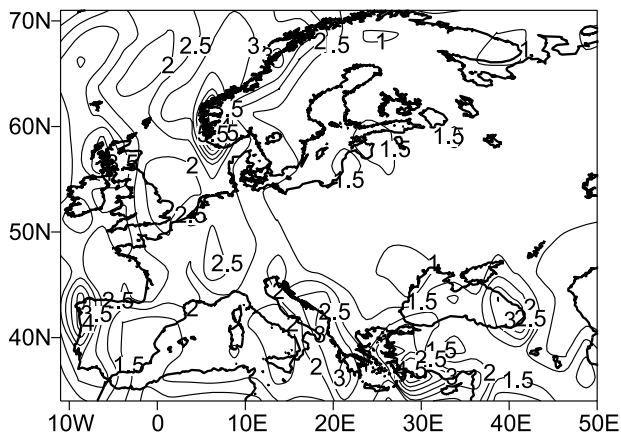
[8] In our analysis we used pentad and monthly precipitation data from the CMAP data set for 1979–2001 [Xie and Arkin, 1996, 1997]. The data were obtained from five kinds of satellite estimates (GOES precipitation index, outgoing longwave radiation-based precipitation index, Special Sensor Microwave Imager (SSM/I) scattering, SSM/I emission, and microwave sounder unit values). This data set consists of pentad and monthly averaged precipitation rate values (mm/d) for the time period January 1979 through December 2001. The data have a 2.5° latitude by 2.5° longitude spatial resolution and cover 88.75°N – 88.75°S and 0°E – 357.5°E . Though these data have a relatively short time history, their advances over other products are the global (including oceanic/marine regions) coverage, and temporal resolution, that provides an opportunity to investigate intraseasonal fluctuations of precipitation along with its interannual variations. Xie and Arkin [1997] note that verification of the CMAP data with a nearly independent gauge data set confirmed their high quality over land areas. The data quality over the oceans is somewhat lower. Nevertheless, the CMAP data are believed to be among the most reliable data on precipitation. In the present study the domain of analysis is limited to latitudes 34°N – 71°N and longitudes 11°W – 50°E .

[9] To verify results obtained from analysis of the CMAP data, we used in this study the CRU05 0.5° latitude/longitude gridded monthly precipitation data [New *et al.*, 1999, 2000]. This data set has been constructed at the Climatic Research Unit, University of East Anglia. The data set represents terrestrial surface climate for the period 1901–1998. This relatively new data set constitutes an advance over other products because (1) it has higher spatial resolution than other data sets of similar temporal extent, (2) it has longer temporal coverage than other products of similar spatial resolution, (3) it encompasses a more extensive suite of surface climate variables than available elsewhere, and (4) the construction method ensures that strict temporal fidelity is maintained. In this study we use precipitation data for the European region that were interpolated directly from station observations. Details on data construction method are given by New *et al.* [1999, 2000]. The limitation of this data set is that by having monthly temporal resolution, it does not permit one to investigate intraseasonal fluctuations of precipitation.

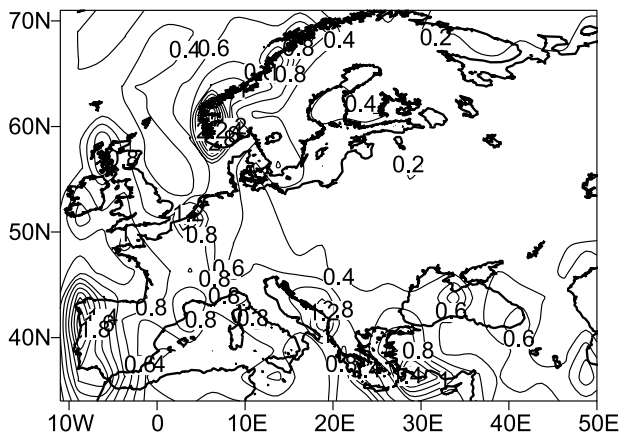
[10] In the present study we also used indices of the major teleconnection patterns that have been documented and described by Barnston and Livezey [1987]. These indices are regularly updated and are available from the Climate Prediction Center (CPC) Web site. The data cover the period 1950 to the present. Details on the teleconnection pattern calculation procedures are given by Barnston and Livezey [1987].

[11] As results of some studies [Fraedrich and Muller, 1992; Dai *et al.*, 1997; Trenberth *et al.*, 1998; Cassou and Terray, 2001] suggest links between European climate variability and El Niño-Southern Oscillation (ENSO), we also use the Southern Oscillation (SOI) and Niño3.4 indices

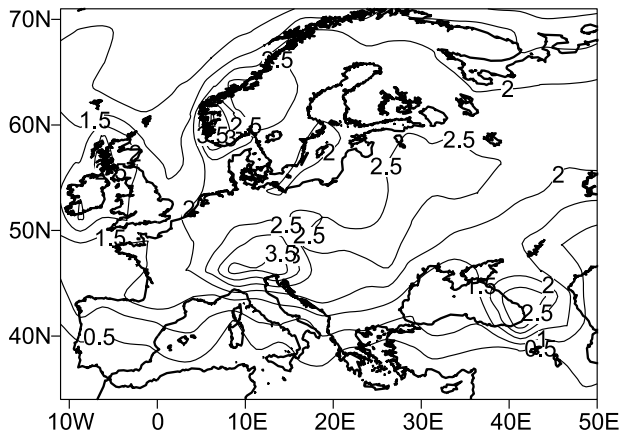
a) Winter (DJF) precipitation climatology



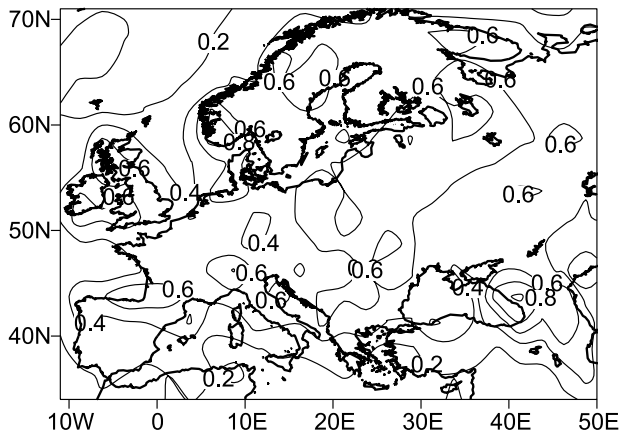
b) Winter (DJF) precipitation STD



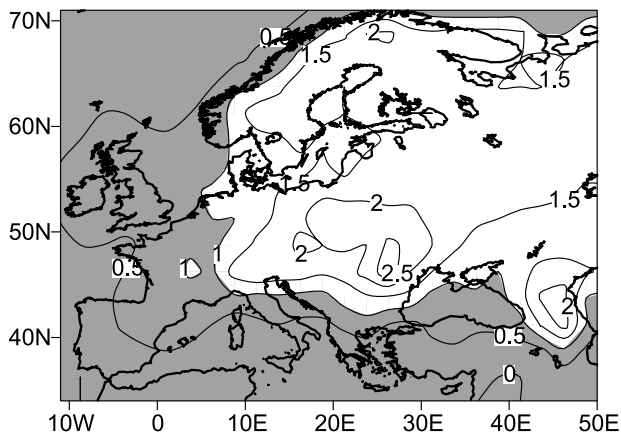
c) Summer (JJA) precipitation climatology



d) Summer (JJA) precipitation STD



e) Ratio JJA/DJF climatologies



f) Ratio JJA/DJF STDs

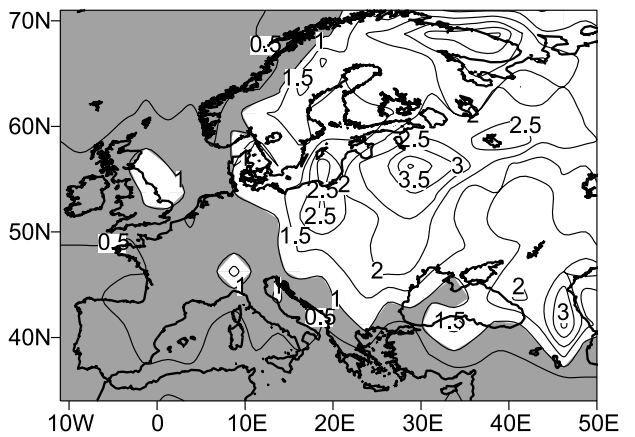


Figure 1. (a and c) Climatologies, (b and d) standard deviations, and (e and f) ratios of the winter (Figures 1a and 1b) and summer (Figures 1c and 1d) CMAP precipitation (1979–2001). Climatologies and standard deviations are presented in mm/d. In Figures 1e and 1f, blue indicates regions where the summer characteristics are lower than the winter ones. See color version of this figure in the HTML.

in the present study. The SOI is defined as the normalized pressure difference between Tahiti and Darwin. There are some slight variations in the SOI values calculated at various centers. Here we use the SOI based on the method given by *Ropelewski and Jones* [1987]. The Niño3.4 index is defined as the sea surface temperature anomalies averaged over the region 5°N – 5°S and 170°W – 120°W . Both the SOI and the Niño3.4 index are available from the CPC Web site.

[12] To reveal dynamical context of some precipitation modes, we used monthly 500 hPa heights data from the National Centers for Environmental Prediction/National Center for Atmospheric Research (NCEP/NCAR) reanalysis [*Kalnay et al.*, 1996]. The NCEP/NCAR reanalysis provides parameters for 6-hourly temporal resolution and 2.5° latitude by 2.5° longitude spatial resolution for a period 1948 to the present. The reanalysis project uses a frozen assimilation technique to analyze past data and gives the possibility to explicitly describe short- and long-term climate variability within the uncertainties introduced by the changes in the input data.

[13] In our study we consider the climatologies of winter (December–January–February (DJF)) and summer (June–July–August (JJA)) seasonal mean precipitation and its standard deviations (SD) as a measure of the total year-to-year variability. We note that over some European regions the maximum precipitation is observed during other seasons. For instance, the climate of the Adriatic Sea and Italy is characterized by the largest precipitation amounts during fall. Therefore our analysis focused on the standard winter and summer seasons has some restrictions. However, it seems that such an approach is reasonable when the domain of analysis is the whole of Europe. Moreover, atmospheric circulation in the Atlantic-European sector (and in midlatitudes in general) is characterized by a pronounced seasonal cycle with stronger (weaker) circulation anomalies during winter (summer) seasons.

[14] To examine spatial-temporal structure of the long-term variations of seasonal mean precipitation over Europe, we applied empirical orthogonal functions (EOF) analysis based on the covariance matrix [*Wilks*, 1995; *von Storch and Navarra*, 1995]. Before the EOF analysis the annual cycle was removed from all grid point time series by subtracting from each seasonal value the respective season's long-term mean. In order to account for the latitudinal distortions, each grid point of the large-scale field anomalies was weighted by the square root of cosine of latitude (φ) to ensure that equal areas are afforded equal weight in the analysis [*North et al.*, 1982]. The long-term stationarity of the time series is preserved for the calculation of EOF through detrending the time series with a linear least square fit. As the time series of the CMAP precipitation are relatively short, we verified robustness of the obtained leading modes of variability by application of the EOF analysis to time series of monthly anomalies of precipitation (i.e., extending time series to $23 \times 3 = 69$ samples). Also, to validate results, we applied EOF analysis to normalized time series of precipitation. Only robust modes of precipitation variability, which were evident in both seasonal and monthly anomalies (as well as in the analysis of the normalized time series), are considered in the paper.

Furthermore, we verified above modes by comparison with the leading modes detected by EOF analysis of the longer time series of precipitation from the CRU data set. Spatial patterns and respective principal components of the leading modes of the CMAP and CRU precipitation are discussed in detail. EOF analysis was also applied to the seasonal standard deviations (estimated on pentad data) that characterize magnitudes of intraseasonal fluctuations of precipitation during a particular season. Though the temporal resolution (pentad) of the data does not allow separation of the different short-term (synoptic) variabilities, we nevertheless believe that standard deviations of the pentad data can be considered as useful indicators of the intensity of intraseasonal fluctuations of precipitation.

[15] To assess links to teleconnection patterns, we used conventional correlation analysis. No lead or lag relationships were taken into consideration for this work; our analysis was restricted to simultaneous connections between winter and summer precipitation fields over Europe and major teleconnection patterns. As we already noted, the limitation of this study is the relatively short record length of the CMAP data. We use the 23-year CMAP precipitation data in this study and rely upon significance tests to evaluate our results. According to the Student's *t*-test [*Bendat and Piersol*, 1966], the minimum significant correlation coefficients between the time series analyzed are 0.413 and 0.526 for the 95% and 99% confidence levels, respectively. Indeed the significance level of the correlation coefficient might be reduced if the time series are influenced by autocorrelation. We checked potential impact of the autocorrelation onto the estimation of significance of correlation coefficients (estimated through the Fisher *z*-transform). Neither time series considered in the study implies significant autocorrelations. Furthermore, to verify assessed links to teleconnection patterns, we analyzed correlations with longer time series of the principal components obtained from the EOF analysis of the rain-gauge-based CRU precipitation data.

3. Interannual Variability of Precipitation

3.1. Climatologies and Standard Deviations of the Seasonal Mean Precipitation

[16] The climatological winter (December–February, hereinafter referred to as DJF) seasonal mean precipitation pattern (Figure 1a) demonstrates high (2–5 mm/d) precipitation over western Europe. Evidently, coastal orography greatly affects the climatology of winter precipitation. Relatively low (1–1.5 mm/day) precipitation is observed over eastern Europe–European Russia. The standard deviation (SD) of the time series of the seasonal mean DJF precipitation is a measure of its year-to-year variability (Figure 1b). This variability is large (0.6–1.8 mm/d) over the regions of maximum precipitation (e.g., western Scandinavia, Portugal), and is lower (0.2–0.4 mm/d) over the regions with low precipitation (Figure 1a). In general, the winter SD pattern is very similar to that of the winter climatology.

[17] Climatology of the summer (June–August, hereinafter referred to as JJA) seasonal mean precipitation over Europe is depicted in Figure 1c. The largest precipitation

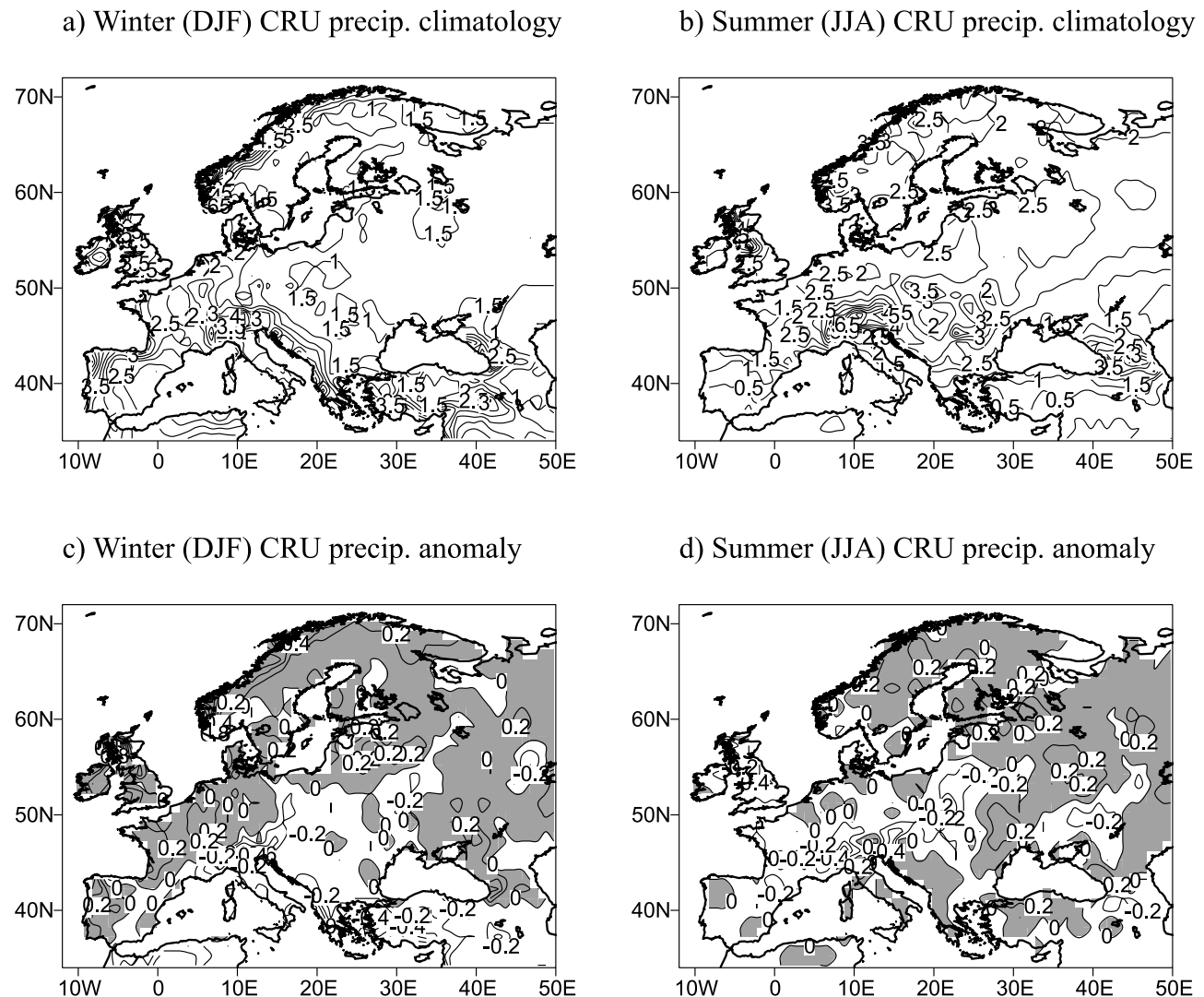


Figure 2. (a and b) Climatologies and (c and d) anomalies of the winter (Figures 2a and 2c) and summer (Figures 2b and 2d) CRU precipitation (1979–1998). Climatologies and anomalies are presented in mm/d. Anomalies are estimated relative to 1901–1978 climatological means. In Figures 2c and 2d, blue indicates negative anomalies. See color version of this figure in the HTML.

amounts, exceeding 2.5 mm/d, are found over the Alps, western Scandinavia, and the Caucasus. Enhanced precipitation is also detected over central eastern Europe. In general, distribution of summer precipitation is more zonal compared to that of the winter season (Figure 1a). Also, the pattern (Figure 1c) features some continentality of the summer precipitation, showing large precipitation over the central part of the region and lower precipitation at the periphery (e.g., Mediterranean region, Scandinavia except its western part). Spatial structure of year-to-year JJA precipitation variability over Europe, presented by its SD, is shown in Figure 1d. The pattern is rather homogeneous and does not reveal significant regional differences. However, effects of orography are evident in this pattern, too. In particular, the largest precipitation variability (presented by SDs reaching 0.8 mm/d) is detected over western Scandinavia, the British Isles, and the Caucasus. Over the major portion of Europe, however, SDs vary in the range 0.4–0.6 mm/d. We note that, in general, SDs of JJA

precipitation over eastern Europe-European Russia are slightly higher compared with those over western Europe.

[18] In order to highlight seasonal differences in precipitation climatologies and SDs, we estimated ratios between respective summer and winter characteristics. Figure 1e shows that over a large portion of Europe (east of 10°E) summer precipitation is essentially higher than that in the winter; specifically over eastern Europe the ratio is as high as 2–2.5. Interannual variability of precipitation over eastern Europe-European Russia is also more intensive during summer season (Figure 1f). The ratios between summer and winter SDs reach values of 2.5–3.5 in this region.

[19] To compare obtained CMAP seasonal climatologies with rain-gauge-based precipitation, we constructed climatologies of winter (DJF) and summer (JJA) seasonal mean precipitation based on CRU monthly precipitation data [New *et al.*, 1999, 2000] for nearly the same period (1979–1998). These climatologies are shown in Figures 2a and 2b. Note that for easier comparison with the CMAP

climatologies, CRU seasonal mean precipitation values were converted from mm/month to mm/d. In general, the CRU climatologies are in a good agreement with the CMAP precipitation climatologies (Figures 1a and 1c), showing larger (smaller) precipitation over western Europe (eastern Europe-European Russia) during winter and smaller (larger) precipitation over western Europe (eastern Europe-European Russia) during the summer season (Figures 2a and 2b). In particular, winter CRU precipitation over eastern Europe-European Russia varies in the range of 1–1.5 mm/d, and winter CMAP precipitation in this region shows very close values (Figure 1a). Summer climatologies (Figures 1c and 2b) of the CMAP and the CRU (2–2.5 mm/d) precipitation are also very close in the region. Differences between the CRU and the CMAP precipitation climatologies are associated with effects of orography. For example, summer CRU precipitation climatology (Figure 2b) reveals a local precipitation maximum over the Carpathians that is not detected in CMAP precipitation (Figure 1c). Also, winter CMAP precipitation climatology (Figure 1a) does not show a precipitation maximum over the Alps that is clearly seen in CRU precipitation (Figure 2a). We believe that the above differences might be attributed to the different spatial resolution in the two data sets. In other words, because of higher spatial resolution the CRU data reflect precipitation maxima associated with orography better than the CMAP data. Different periods (1979–2001 for CMAP and 1979–1998 for CRU data) of averaging also may play some role. In contrast to the CRU data, the CMAP data set provides information on precipitation over the Mediterranean Sea (and other marine/oceanic regions). Seasonal precipitation climatologies demonstrate remarkable differences in this region. The summer precipitation climatology (Figure 1c) is characterized by almost zonal distribution of precipitation over the Mediterranean Sea with its gradual increase in a south-north direction. Unlike the summer precipitation, winter precipitation climatology (Figure 1a) reveals well-pronounced local maximum of precipitation over eastern Mediterranean.

[20] Figures 2c and 2d show seasonal CRU precipitation anomalies for 1979–1998, relative to climatologies estimated for 1901–1978. The present patterns reflect changes in winter and summer precipitation climatologies during the last 2 decades (period of the present analysis) of the twentieth century. For the winter season (Figure 2c), precipitation decreased over Italy and the eastern Mediterranean region, whereas an increase of winter precipitation is evident in other parts of the European continent. Summer precipitation decreased over the British Isles and most of western, central, and eastern Europe (Figure 2d). An increase of summer precipitation is detected over Italy, the eastern Mediterranean, Scandinavia, and most of European Russia. It is interesting to note the opposite tendencies of precipitation changes in some regions for winter and summer seasons. For instance, winter precipitation increased over the British Isles, while summer precipitation decreased in this region. On the other hand, decreases in winter and increases in summer precipitation are detected over Italy and the eastern Mediterranean region (Figures 2c and 2d). These opposite tendencies reflect seasonality of the long-term precipitation changes over the above regions. In

general, our analysis shows that climatologies of precipitation over Europe changed during the last decades, and the changes are different for winter and summer precipitation.

3.2. Leading Modes of Interannual Precipitation Variations

[21] In order to reveal leading modes of interannual variability of precipitation over Europe, we performed EOF analysis on time series of the winter and summer seasonal mean precipitation from CMAP for the period 1979–2001. Spatial patterns of the first two EOF modes of DJF precipitation and time series of the corresponding principal components are shown in Figure 3.

[22] The first EOF mode accounts for 42.1% of the total variance of winter precipitation. The respective spatial pattern (Figure 3a) shows two major anomaly centers of opposite polarity over Scandinavia and the Mediterranean region. In general, this pattern reflects opposite DJF precipitation changes over northern and southern Europe, and these changes are more pronounced over the western (west of 20°E) portion of the region. The time series of the corresponding principal components (Figure 3c) display the temporal behavior of this mode. In particular, anomalously wet (dry) conditions over southern (northern) Europe in 1996 and 2001 are well captured. This mode is linked to the major climatic signal in the region, the North Atlantic Oscillation (NAO). Details of this linkage will be discussed in section 5.

[23] The second EOF mode explains 16.2% of the total variance of DJF precipitation. The respective spatial pattern (Figure 3b) is characterized by three anomaly centers. The pattern reflects coherent precipitation variations over the Mediterranean region and northwestern Scandinavia and opposite variations over the rest part of Europe. We note that like in the case of the first EOF mode, variability expressed by the second EOF mode is concentrated mostly in the western (west of 20°E) portion of the region. Time series of the corresponding principal components display the temporal behavior of this mode (Figure 3d), characterized by the enhanced (compared with the 1980s) interannual variations of precipitation during the last decade of the twentieth century. Taking into account precipitation variance explained by the second EOF mode, we note that its effect on precipitation anomalies, in general, may not be very strong. However, the local effect of this mode might be essential in the regions characterized by the large loadings (e.g., the British Isles). As will be discussed in section 5, the second EOF mode of DJF precipitation over Europe might be associated with the East Atlantic teleconnection pattern that was described by Barnston and Livezey [1987].

[24] For the summer (JJA) CMAP precipitation, only the first EOF mode is statistically well separated according to the test of North *et al.* [1982]. The spatial pattern of the first EOF mode of JJA precipitation and time series of the corresponding principal components are shown in Figure 4. The first EOF mode accounts for 25.5% of the total variance of summer precipitation. The spatial pattern reveals three anomaly centers: over the southern Europe/Mediterranean region, a major portion of Europe north of 45°N, and a minor anomaly center over northeastern Scandinavia (Figure 4a). While the variation of JJA precipitation over the southern Europe/Mediterranean region and northeastern Scandinavia

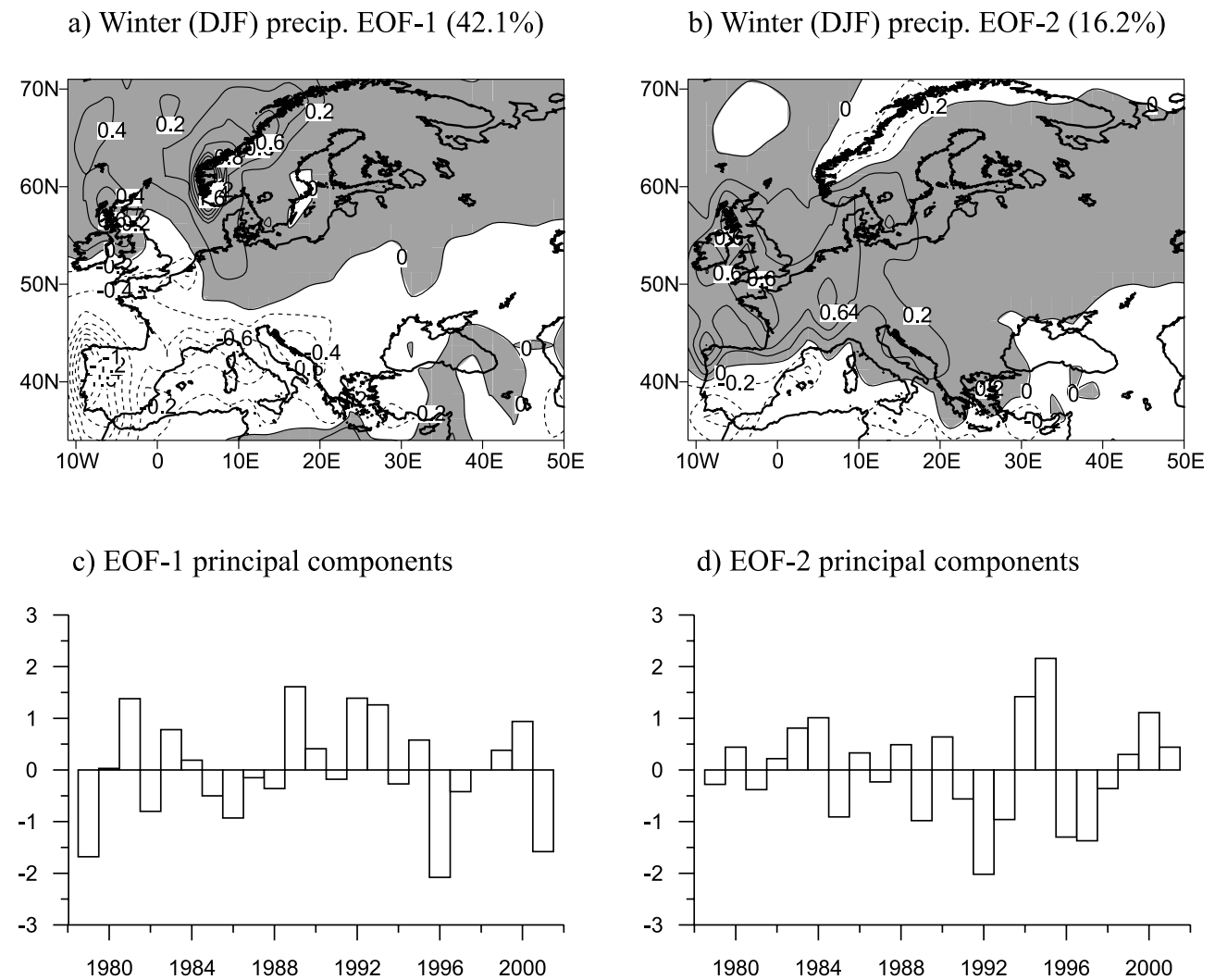


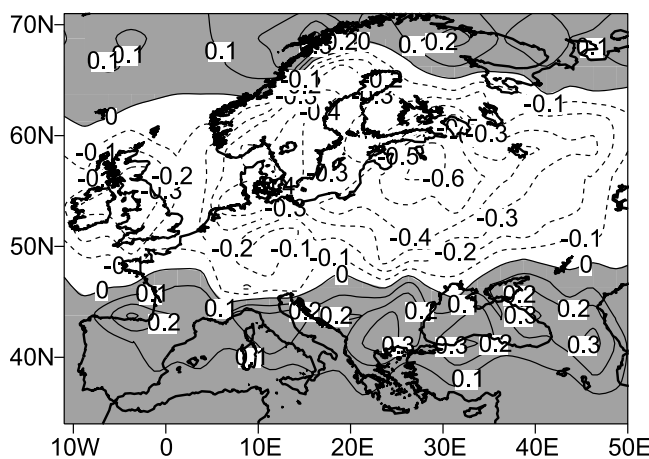
Figure 3. (a and b) Spatial patterns and (c and d) the respective principal components of the first two EOF modes of the winter CMAP precipitation (1979–2001). Principal components are normalized by their standard deviations. Blue indicates negative values. See color version of this figure in the HTML.

is in phase, it is opposite to that over a large portion of Europe. It is important to note that in contrast to the first EOF mode of DJF precipitation (where large variability is observed mostly over western Europe), this pattern reflects precipitation variations over the whole of Europe. During recent decades the corresponding principal components (Figure 4b) of this mode demonstrate distinct multiyear periods of positive (1981–1984, 1994–1997) and negative (1985–1990) anomalies. This feature of decadal scale variability is also evident in summer (July–August) time series of sea level pressure over northeast Atlantic presented by *Hurrell and Folland* [2002, Figure 1]. Though the first EOF mode of JJA precipitation is associated with the summertime NAO (which will be shown in section 5), its temporal behavior is principally different from that of the first EOF mode of DJF precipitation. Further analysis has shown that the time series of respective principal components are not correlated (correlation coefficient is 0.07). It is also worth noting that the spatial pattern of the summer NAO is essentially different from that of the winter NAO [*Barnston and Livezey*, 1987].

[25] To verify results obtained from analysis of the relatively short time series of the CMAP precipitation, we performed EOF analysis on the longer time series of the winter and summer seasonal mean precipitation from the CRU data set for the period 1958–1998. Spatial patterns of the first two EOF modes of DJF precipitation and time series of the corresponding principal components are shown in Figure 5.

[26] The first EOF mode accounts for 30.2% of the total variance of the CRU winter precipitation. The spatial pattern of this mode (Figure 5a) is similar to that obtained for the CMAP precipitation (Figure 3a) and shows two major anomaly centers of opposite polarity over Scandinavia and the Mediterranean region. The time series of the corresponding principal components (Figure 5c) also show temporal behavior similar to that of the first EOF mode of the winter CMAP precipitation (Figure 3c). Correlation between respective time series during overlapping time periods (1979–1998) is very high (0.98) and statistically significant at the 99% confidence level according to Student's *t*-test [*Bendat and Piersol*, 1966]. We note that

a) Summer (JJA) precip. EOF-1 (25.5%)



b) EOF-1 principal components

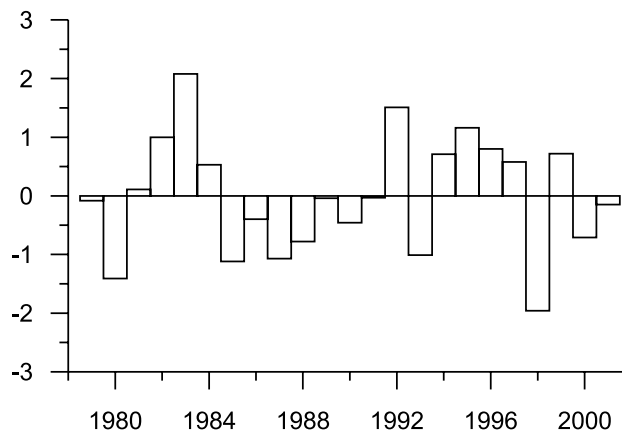


Figure 4. (a) Spatial pattern and (b) the respective principal components of the first EOF mode of the summer CMAP precipitation (1979–2001). Principal components are normalized by their standard deviations. Blue indicates negative values. See color version of this figure in the HTML.

compared with the first EOF mode of the CMAP precipitation, this mode explains a lower percentage of the winter precipitation variance. Because the first EOF mode of the winter precipitation over Europe is associated with the NAO, and because the last decades of the twentieth century were characterized by the enhanced NAO, detected differences in the explained variances are somewhat expected.

[27] The second EOF mode explains 17.0% of the total variance of the CRU winter precipitation. Note that the explained variance is very close to that of the second EOF mode of the CMAP precipitation (16.2%). Like in the case of the first EOF mode, the respective spatial pattern (Figure 5b) is similar to the pattern obtained for the second EOF mode of the CMAP winter precipitation (Figure 3b). It is characterized by three anomaly centers and reflects coherent precipitation variations over the Mediterranean

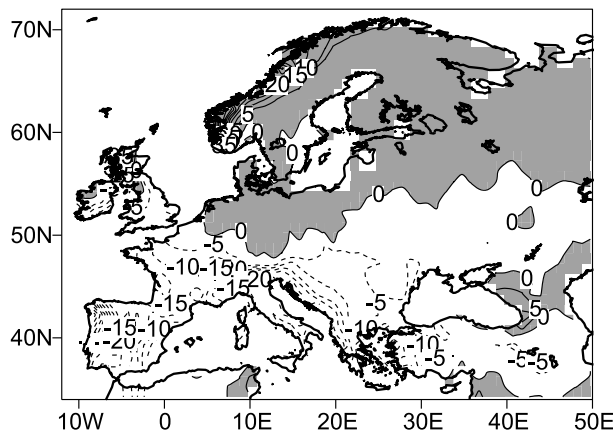
region and northwestern Scandinavia and opposite variations over the rest part of Europe. Time series of the corresponding principal components (Figure 5d) display temporal behavior similar to that of the second EOF mode of the CMAP winter precipitation (Figure 3d). Correlation between respective time series during the overlapping time period (1979–1998) is also very high (0.95) and statistically significant at the 99% confidence level. Therefore the second EOF of the CRU winter precipitation is the same mode that was revealed by EOF analysis of the shorter time series of the CMAP precipitation.

[28] In contrast to the CMAP precipitation, EOF analysis of the longer time series of the CRU summer precipitation revealed two statistically significant modes of its variability. Spatial patterns of these two EOF modes of the CRU summer precipitation and time series of the corresponding principal components are shown in Figure 6. The first EOF mode accounts for 17.6% of the total variance of summer precipitation. Its spatial pattern (Figure 6a) is similar to that of the first EOF mode of the CMAP summer precipitation (Figure 4a) and reveals three anomaly centers: over the southern Europe/Mediterranean region, a major portion of Europe north of 45°N, and a minor anomaly center over northern Scandinavia. Note that along with those detected in the CMAP precipitation multiyear periods of positive and negative anomalies (Figure 4c), the corresponding principal components (Figure 6c) of this mode also reveal a period of predominantly positive anomalies during 1967–1977. Thus this mode features decadal-scale variability in summer precipitation over Europe. Correlation between principal components of this mode and those of the first EOF mode of the CMAP summer precipitation during the overlapping time period (1979–1998) is very high (0.97) and statistically significant at the 99% confidence level.

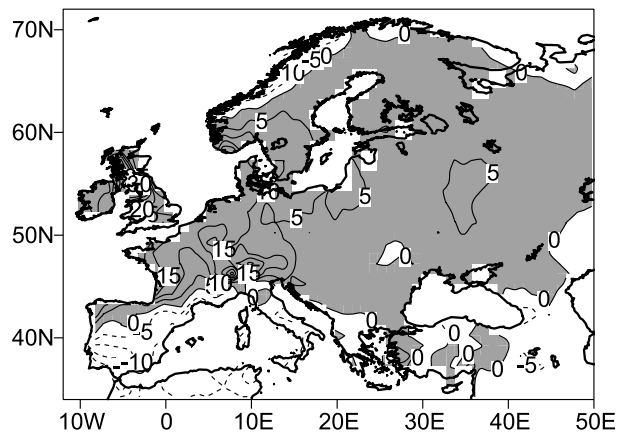
[29] The second EOF mode of the CRU summer precipitation explains 13.2% of its total variance. The spatial pattern of this mode (Figure 6b) is characterized by the opposite precipitation variations over northeastern Europe and over the large portion of Europe south of approximately 55°N. A very weak third anomaly center is seen over southern Italy and the Balkans, where variations of precipitation are coherent with those over northeastern Europe. Compared with the first EOF mode (Figure 6c), principal components of this mode (Figure 6d) display precipitation variability at higher frequencies. Power spectrum for this time series and the 95% confidence limit of the red noise spectrum are presented in Figure 7. The Parzen lag window is used to smooth the sample spectrum [Chu and Katz, 1989]. The power spectrum of the second EOF mode of the CRU summer precipitation (Figure 7) shows that only variations with a time period 2.5–3 years are statistically significant. It is worth noting that a similar (in terms of spatial structure and temporal behavior) mode was revealed by EOF analysis of the CMAP summer precipitation. However, it was not well separated from other modes according to the test of North *et al.* [1982].

[30] Thus the leading EOF modes of the winter and summer precipitation over Europe detected in the CMAP data are also revealed by EOF analysis of the longer time series of the rain-gauge-based CRU precipitation. We note that the EOF analysis of the century-long (1901–1998) time series (not shown) of the CRU precipitation also revealed

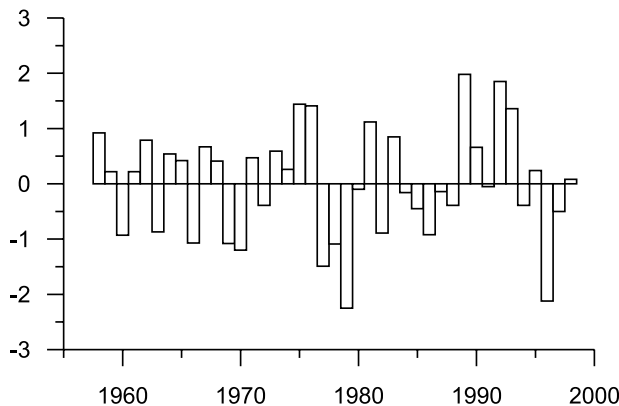
a) Winter CRU precip. EOF-1 (30.2%)



b) Winter CRU precip. EOF-2 (17.0%)



c) EOF-1 principal components



d) EOF-2 principal components

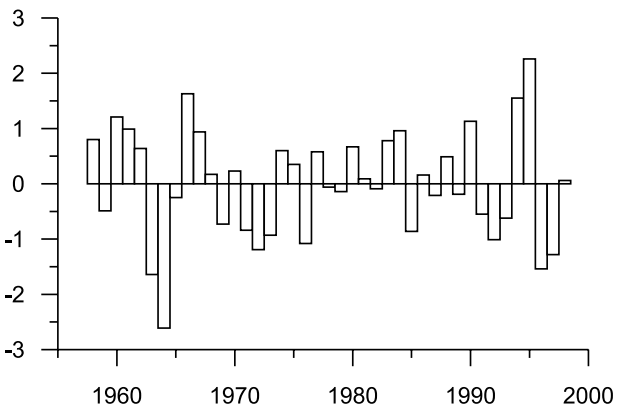


Figure 5. (a and b) Spatial patterns and (c and d) the respective principal components of the first two EOF modes of the winter CRU precipitation (1958–1998). Principal components are normalized by their standard deviations. Blue indicates negative values. See color version of this figure in the HTML.

leading EOF modes, characterized by spatial structures and temporal behavior similar to those described above. However, explained variances in that analysis are, in general, lower than those obtained for the shorter periods of analysis. This is somewhat expected because longer time series present a wider range of timescales of precipitation variability.

4. Intraseasonal Fluctuations of Precipitation

4.1. Standard Deviations of the Pentad Mean Precipitation

[31] To characterize the intensity (or magnitude) of intraseasonal fluctuations of precipitation over Europe, we estimated standard deviations of pentad precipitation for each winter and summer season. In order to make a distinction between standard deviations of seasonal means and those of pentad precipitation, we further refer to the latter as the magnitudes of intraseasonal fluctuations (hereinafter referred to as MGN). On the basis of obtained time

series of MGN, climatologies and interannual standard deviations of the winter (DJF) and summer (JJA) MGN of precipitation were estimated.

[32] The climatological winter MGN pattern over Europe (Figure 8a) demonstrates very high (2–2.5 mm/day) magnitudes of intraseasonal fluctuations of precipitation over western Europe (west of 20°E) and over the southeastern Mediterranean Sea and the Black Sea. Magnitudes of intraseasonal fluctuations of precipitation over eastern European Russia are relatively low (about 1 mm/d). It is evident that intraseasonal fluctuations of precipitation over Europe are affected substantially by orography. In general, there is good agreement between winter seasonal mean climatology and interannual SDs (Figures 1a and 1b) and magnitudes of intraseasonal fluctuations of precipitation (Figure 8a). Also, it is important to note that magnitudes of intraseasonal fluctuations are essentially higher than those of interannual variations (Figure 1b). The SDs of the time series of winter MGN reflect their year-to-year variability (Figure 8b). In contrast to climatology (Figure 8a), SDs of

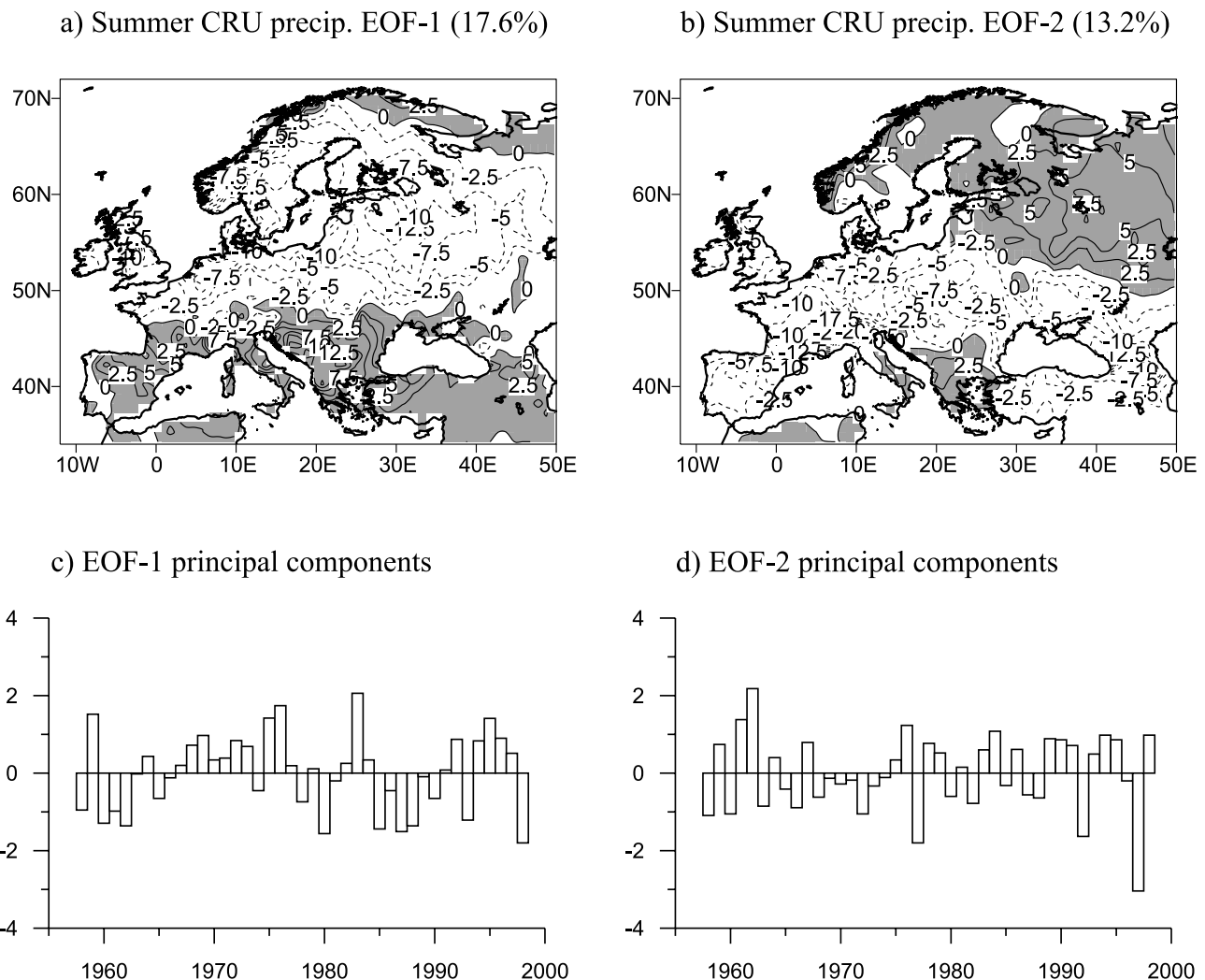


Figure 6. (a and b) Spatial patterns and (c and d) the respective principal components of the first two EOF modes of the summer CRU precipitation (1958–1998). Principal components are normalized by their standard deviations. Blue indicates negative values. See color version of this figure in the HTML.

interannual variability of winter MGN (0.4–0.6 mm/d) over eastern Europe-European Russia are comparable to those over western Europe.

[33] Figure 8c shows the climatology of the summer MGN of precipitation over Europe. The largest intra-seasonal fluctuations of precipitation with the MGN values reaching 2.5 mm/d are found over the Alps, western Scandinavia, and the Caucasus. Similar to the seasonal mean summer precipitation climatology (Figure 1c), the climatological distribution of summer MGN of precipitation reflects, in general, enhanced intra-seasonal fluctuations of precipitation over central eastern Europe (Figure 8c). The spatial structure of the JJA MGN of precipitation year-to-year variability over Europe, presented by their SDs, is shown in Figure 8d. The pattern demonstrates stronger interannual variations of MGN over eastern Europe-European Russia compared with those over western Europe. It is interesting to note that in this region, magnitudes (0.6–1.2 mm/d) of these variations are also larger than those obtained for the winter season (Figure 8b).

[34] Estimated ratios between summer and winter climatologies of MGN and between respective interannual SDs are present in Figures 8e and 8f. Over western Europe (west of 10°E), summer magnitudes of intra-seasonal fluctuations of precipitation and their interannual SDs are lower than those of the winter season. Over eastern Europe-European Russia, however, summer MGN climatologies and their interannual SDs exceed those of the winter season by an order of 2 or more (Figures 8e and 8f). In general, the present ratio patterns are in a good agreement with the ratios estimated for seasonal mean precipitation climatologies and their interannual SDs (Figures 1e and 1f).

4.2. Leading Modes of Interannual Variations of the Magnitudes of Intraseasonal Precipitation Fluctuations

[35] To investigate leading modes of year-to-year variations in the magnitudes of intra-seasonal fluctuations of precipitation over Europe, we applied EOF analysis to time series of MGN of precipitation (1979–2001) estimated for winter and summer seasons. For the winter

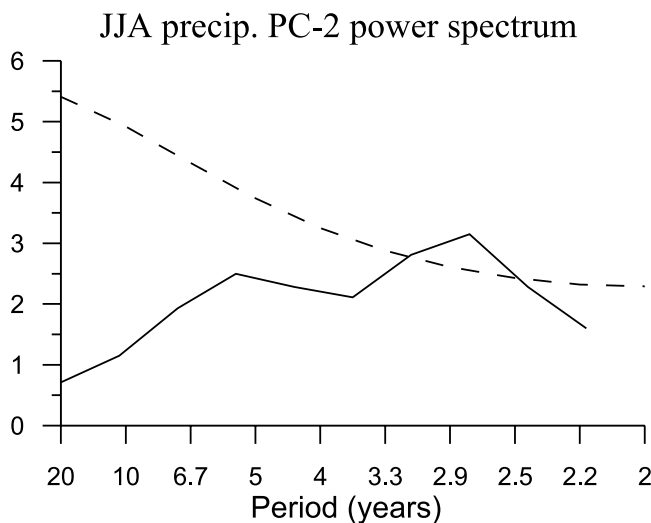


Figure 7. Power spectrum of the EOF-2 principal components of the summer CRU precipitation. Dashed curve is the 95% significance level of the red noise spectrum.

season, only the first EOF mode is separated reasonably well with respect to sampling errors [North *et al.*, 1982]. Though the second EOF mode is marginally significant, it is strongly biased by the very large loadings over very small regions (e.g., the Caspian Sea region). Thus we consider only the first EOF mode. The spatial pattern of the first EOF mode for DJF MGN of precipitation and time series of the corresponding principal components are shown in Figure 9.

[36] The first EOF mode accounts for 21.4% of the total variance of the winter MGN of precipitation. The respective spatial pattern (Figure 9a) shows two major anomaly centers of opposite polarity over western Scandinavia and the Mediterranean region. Although there are some differences over eastern Europe-European Russia, a very close agreement with the first EOF mode of seasonal mean DJF precipitation (Figure 3a) over western (west of 20°E) Europe is remarkable. Hence, at the timescale of the first EOF mode, variations of seasonal mean DJF precipitation are strongly linked to changes in the magnitudes of intraseasonal fluctuations of precipitation. In other words, enhanced (reduced) DJF precipitation is associated with enhanced (reduced) MGN of precipitation during the winter season. Time series of the corresponding principal components (Figure 9c) depict the temporal behavior of this mode. Evidently, this mode is linked to the wintertime NAO and to the first EOF mode of DJF precipitation. These links will be discussed in detail in section 5.

[37] For the summer season, EOF analysis of the MGN of precipitation did not reveal statistically significant modes of variability. Although EOF analysis of the monthly (JJA) time series of the MGN of precipitation revealed a marginally significant first EOF mode, it seems that this mode is not robust. Therefore we do not consider this mode in the present study. Nevertheless, it is worth noting that our analysis did not reveal links between this mode and the detected EOF modes of seasonal mean summer precipita-

tion. It also appeared that this mode is not associated with the summertime NAO.

5. Links to Teleconnection Patterns

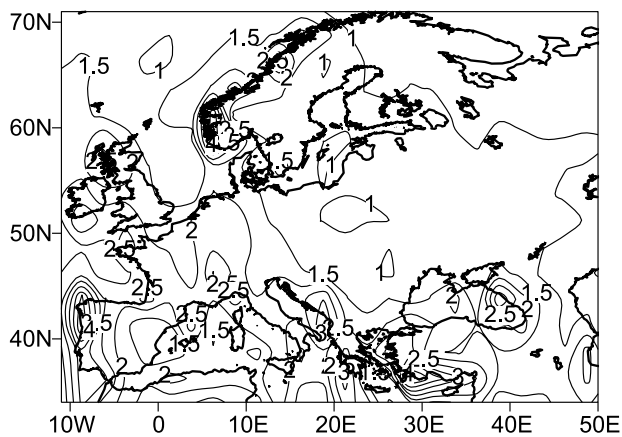
[38] In this section, on the basis of conventional correlation analysis, we examine and briefly discuss links between revealed leading modes of seasonal means and magnitudes of intraseasonal fluctuations of precipitation, and major teleconnection patterns. Correlations with various (e.g., East Atlantic Jet pattern, Scandinavia pattern, Polar/Eurasia pattern, etc.) teleconnection patterns were estimated. However, we consider only those patterns that demonstrated significant correlations with the leading modes of precipitation variability over Europe. We note that established links were confirmed by analysis of the correlations between longer time series of the CRU precipitation and teleconnection patterns (not shown). Table 1 presents respective correlations estimated for the winter and summer seasons.

[39] During winter the first EOF modes of both seasonal mean precipitation and the MGN of precipitation are strongly linked to the NAO. Respective correlations of 0.63 and 0.64 are statistically significant at the 99% confidence level according to the *t*-test [Bendat and Piersol, 1966]. Naturally, correlation between corresponding principal components is also high (0.72) and statistically significant. Altogether, that means the high NAO index (i.e., positive phase of the NAO) results in enhanced intraseasonal fluctuations and excessive winter precipitation over northern Europe and decreased intraseasonal fluctuations and deficient precipitation over southern Europe. Opposite anomalies in the magnitudes of intraseasonal fluctuations and in the seasonal mean DJF precipitation are observed when the NAO index is low (i.e., negative phase of the NAO). It is known that there is a connection between the seasonally averaged NAO and low-frequency variability within a season over the Atlantic [Nakamura, 1996]. As shown in recent studies [Rogers, 1990, 1997; Beniston, 1997; Appenzeller *et al.*, 1998], changes in the mean atmospheric circulation over the North Atlantic are accompanied by pronounced shifts in the storm tracks and associated synoptic eddy activity. These changes affect the transport and convergence of atmospheric moisture and can be directly linked to changes in regional precipitation. Therefore our results confirm that such links do exist and are robust.

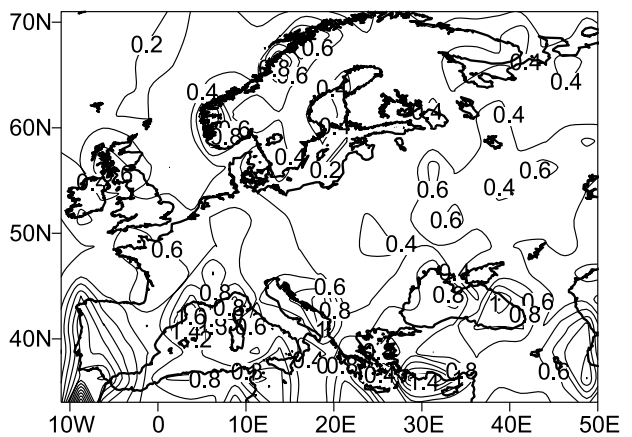
[40] The second EOF mode of DJF precipitation might be associated with the East Atlantic (EA) teleconnection pattern. Correlation between respective time series (Table 1) is 0.5, which is statistically significant at the 95% confidence level according to the *t*-test [Bendat and Piersol, 1966]. The respective EA-associated EOF mode in the DJF MGN of precipitation, however, is not revealed by the present analysis. Although the ENSO reaches its mature phase during boreal winter, we did not find statistically significant links between DJF precipitation variability over Europe and ENSO.

[41] Table 1 also shows correlations between leading EOF modes of the summer seasonal mean precipitation and major teleconnection patterns. During summer, the first EOF mode of seasonal mean precipitation is strongly linked to the summer NAO. Correlation (0.81) between principal

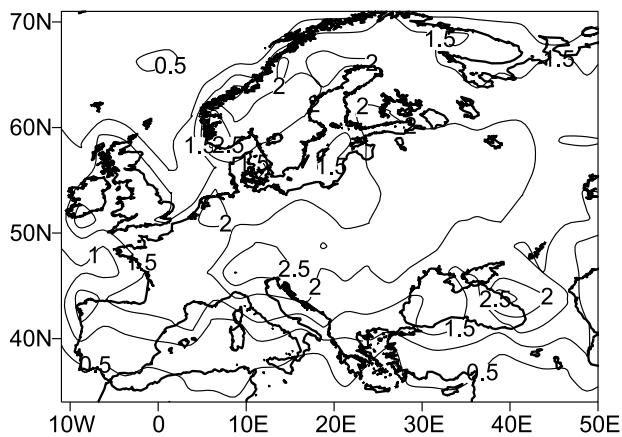
a) Winter MGN precipitation climatology



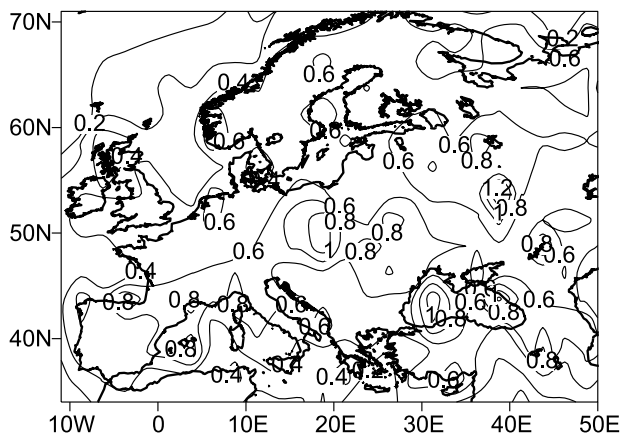
b) Winter MGN precipitation STD



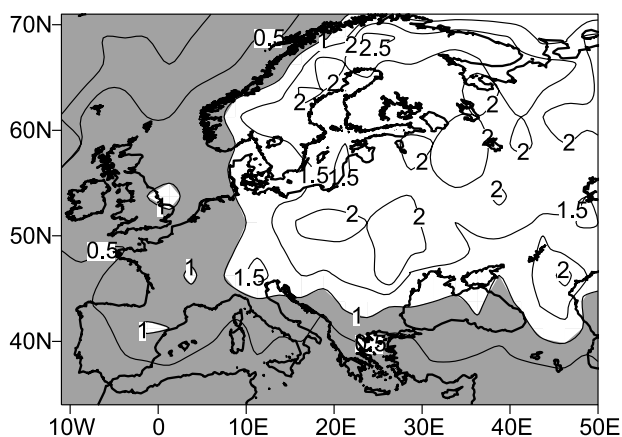
c) Summer MGN precipitation climatology



d) Summer MGN precipitation STD



e) Ratio summer/winter MGN pre. clim.



f) Ratio summer/winter MGN pre. STDs

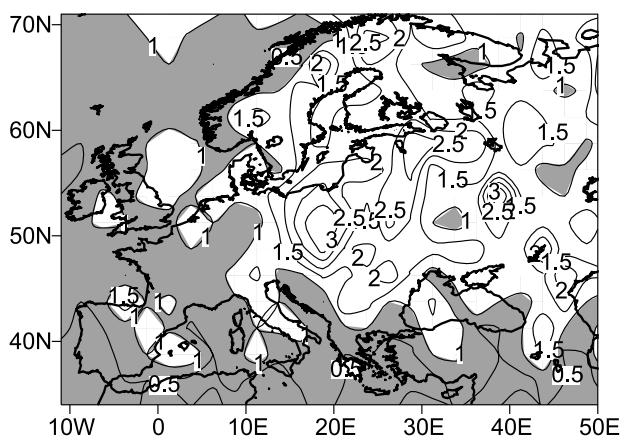


Figure 8. (a and c) Climatologies, (b and d) standard deviations, and (e and f) ratios of the winter (Figures 8a and 8b) and summer (Figures 8c and 8d) MGN of the CMAP precipitation (1979–2001). Climatologies and standard deviations of MGN are presented in mm/d. In Figures 8e and 8f, blue indicates regions where the summer characteristics are lower than the winter ones. See color version of this figure in the HTML.

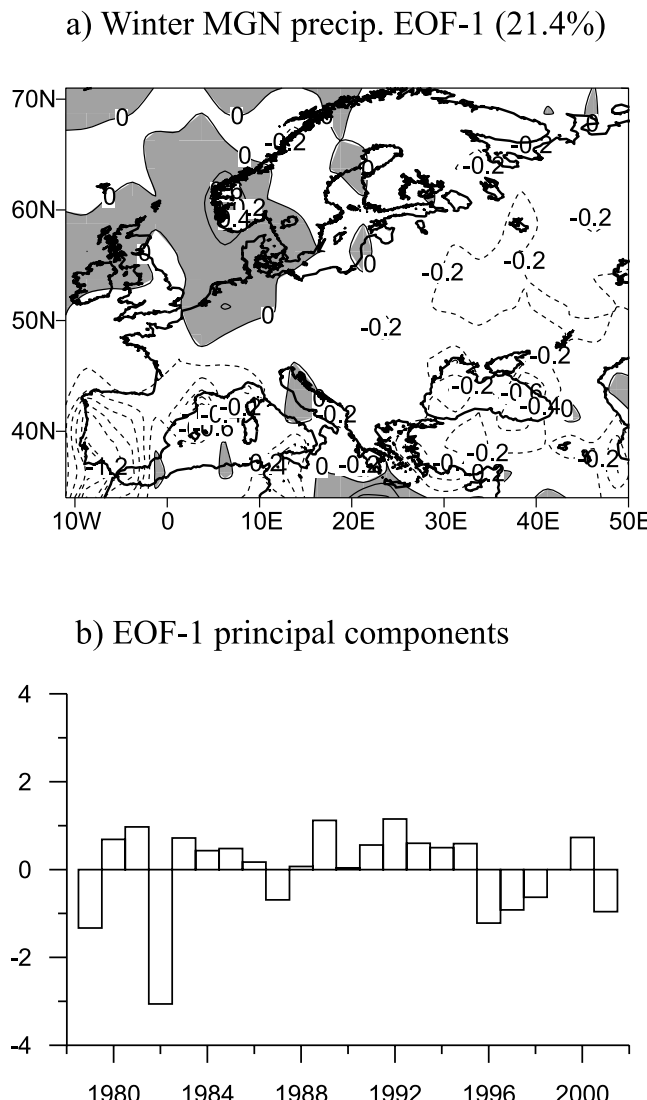


Figure 9. (a) Spatial pattern and (b) the respective principal components of the first EOF mode of the winter MGN of the CMAP precipitation (1979–2001). Principal components are normalized by their standard deviations. Blue indicates negative values. See color version of this figure in the HTML.

components of this mode and the NAO index is even stronger than that obtained for the winter season (0.63). That means a high summer NAO index (i.e., positive phase of the NAO) leads to excessive precipitation over southern Europe/Mediterranean region and northeastern Scandinavia,

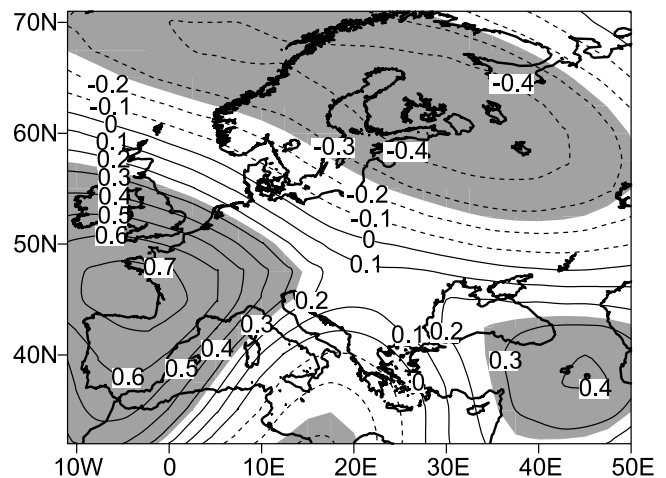


Figure 10. Correlation coefficients between EOF-2 principal components of the summer CRU precipitation and 500 hPa height anomalies. Shaded areas indicate the 95% significance level.

and deficient precipitation over central Europe-European Russia. Low NAO index (i.e., negative phase of the NAO) results in opposite anomalies in the seasonal mean JJA precipitation over Europe. As we already noted, the marginally significant (and not considered in the present study) first EOF mode of the monthly (JJA) MGN of precipitation is not linked to the summer NAO.

[42] The second EOF mode of JJA precipitation (revealed in the CRU data) does not show statistically significant correlations with the known teleconnection patterns (Table 1). To show the dynamical context of this precipitation mode, we performed the correlation analysis between the time series of PC-2 of JJA precipitation and 500 hPa height anomalies. The correlation pattern is shown in Figure 10. The pattern reveals four anomaly centers: two major centers of opposite polarity over western Europe and Scandinavia-northeastern European Russia, and two minor centers over central southern Mediterranean region and the Caucasus. In general, this pattern implies that positive/negative (i.e., anticyclonic/cyclonic) anomalies in the 500 hPa heights result in negative/positive precipitation anomalies in the respective regions. It is worth noting that this mode might also represent a lagged response in summer precipitation over Europe to some remote or local signal in the climate system.

6. Summary and Discussion

[43] We analyzed the climatic variability of precipitation over Europe based on data from the CMAP [Xie and Arkin,

Table 1. Correlation Coefficients Between Leading Modes of Winter and Summer Seasonal Mean Precipitation (WINPC and SUMPC), Magnitudes of Intraseasonal Fluctuations (MGNWPC), and Teleconnection Patterns^a

	Winter			Summer	
	WINPC-1	WINPC-2	MGNWPC-1	SUMPC-1	SUMPC-2
MGNWPC-1	0.72	0.07	...	NAOs	0.81
NAO _W	0.63	0.39	0.64		0.10
EA _W	-0.04	0.50	-0.07		

^aCoefficients that are significant at the 99% and 95% confidence levels are present in bold and italic, respectively.

1996, 1997] and the CRU [New *et al.*, 1999, 2000] data sets. Special emphasis in this study is made on the seasonality of precipitation variations at the different timescales. Intercomparison of the seasonal climatologies (estimated for the last 2 decades of the twentieth century) and characteristics of precipitation variability showed a good general agreement between the two data sets. It is also shown that climatologies of precipitation of the late twentieth century differ from those estimated for the earlier periods of observations. Therefore comparison of the CMAP seasonal precipitation climatologies (1979–2001) with earlier constructed ones [Korzun *et al.*, 1978; Legates, 1987; Legates and Willmott, 1990] would not be correct, and quantitative agreement with those climatologies is not expected. In particular, Legates and Willmott [1990] noted that their precipitation climatology is largely representative of the 60-year period 1920–1980. Korzun *et al.*'s [1978] precipitation climatology is also constructed for the pre-CMAP period of observations. Moreover, differences in climatologies might be associated not only with the different periods of averaging, but also with the gridding procedures (that generally reduce variances) used in the construction of the modern data sets, and with gauge instrumental adjustments that were used in the earlier climatologies [Korzun *et al.*, 1978; Legates, 1987], but were not applied in the data sets used in the present study.

[44] Apparent seasonal differences are detected both in precipitation climatologies and in characteristics of its variability. Over western Europe the summer precipitation climatology and year-to-year variations (expressed by SDs) of precipitation are lower than those of the winter precipitation. Major seasonal differences are detected over central eastern Europe and European Russia. In this region, summer precipitation climatology and magnitudes of interannual variability of precipitation exceed respective winter characteristics by a factor of 2–3.5. Similar relationships are found for the summer and winter magnitudes of intraseasonal fluctuations of precipitation. In particular, over eastern Europe-European Russia, summer MGN climatologies and their interannual SDs exceed those of the winter season by an order of 2 or more.

[45] The leading EOF modes of both seasonal mean precipitation and magnitudes of intraseasonal fluctuations are clearly season-dependent. Although the first EOF modes of the winter and summer precipitation are both associated with the NAO, they are characterized by the principally different spatial patterns and by different temporal behavior. They also explain remarkably different amounts of the total precipitation variance. Compared with the first EOF mode of the winter precipitation, the first EOF mode of the summer precipitation features longer decadal-scale variations. As we noted earlier, these variations in the summer seasonal mean precipitation are consistent with those detected in sea level pressure over the northeast Atlantic by Hurrell and Folland [2002]. It is important to note that in the present study we used NAO indices defined by the rotated principal component analysis of the 700 hPa height anomalies [Barnston and Livezey, 1987]. This point is crucial for the present study because such an approach provides deeper insight into the seasonality of the dominant modes. Several studies [Blasing, 1979, 1981; Portis *et al.*, 2001] have revealed essential seasonal differences in long-

term variability of the NAO. In particular, Blasing [1979, 1981] found the period from 1900 to 1920 to be characterized by a negative NAO pattern in summer and positive NAO pattern in winter. In contrast to that, during the 1930–1955 period summer (winter) was characterized by a positive (negative) NAO pattern. It is worth noting that Barnston and Livezey [1987] obtained essentially different spatial patterns for the winter and summer NAO (see, for example, their Figures 2a and 2g). Therefore it is not surprising that both being associated with the NAO, the first EOF modes of the summer and winter precipitation are characterized by principally different spatial patterns and very different temporal behavior.

[46] We believe there are two major factors responsible for the above differences in winter and summer precipitation variations. The first factor is the seasonal displacements of the NAO anomaly centers. While the winter NAO is represented by the well-known meridional dipole pattern over the North Atlantic [Hurrell, 1995], the summer NAO (in its positive phase) is characterized by a positive (anticyclonic) pressure anomaly over central Europe and by negative (cyclonic) anomalies over Greenland and northern seas, and over the Mediterranean Sea (see Barnston and Livezey [1987] or the respective pattern at the CPC Web site). This results in deficient precipitation over central Europe and excessive precipitation over northern Scandinavia and the Mediterranean region. The reversed picture is observed during the negative phase of the summer NAO. Therefore, during the summer season, excessive (deficient) precipitation over central Europe-eastern Europe is associated with the negative (positive) phase of the NAO. The second important factor is the “recycling” ratio (i.e., the ratio of how much precipitation comes from a local region through evaporation versus how much comes from advection into the region). It was shown that the recycling ratio varies substantially from lower values in winter to higher values in summer, when the large-scale transports diminish in importance [Trenberth, 1999; Trenberth *et al.*, 2003]. In particular, estimates of Trenberth [1999] show essential seasonal increase of the recycling ratio values over southern and southeastern Europe. Thus local evaporation plays a more important role (compared with winter) in the formation of summer precipitation in the region and may be (at least partly) responsible for the detected seasonal differences in precipitation variability over Europe. In this respect, study of the seasonally varying influence of the Mediterranean Sea heat fluxes on precipitation over Europe would also be of great interest.

[47] The second EOF mode of the seasonal mean winter precipitation is associated with the East Atlantic (EA) teleconnection pattern, detected and described by Barnston and Livezey [1987]. The EA pattern is similar to the NAO and characterized by a meridional dipole of two anomaly centers, but the EA action centers are displaced southeastward relative to those of the NAO pattern. Another distinction between the NAO and EA patterns is a strong subtropical link of the lower-latitude action center of the EA pattern. In contrast with the first EOF mode, our analysis did not reveal an EA-associated mode in the magnitudes of intraseasonal fluctuations of the winter precipitation.

[48] A statistically significant second EOF mode of the seasonal mean summer precipitation has been revealed only

in the longer time series of the CRU precipitation. As we already noted, we did not find significant correlations between this mode and known teleconnection patterns. Correlations between principal components of this mode and 500 hPa height anomalies formed the pattern, which is characterized by four anomaly centers: two major centers of opposite polarity over western Europe and Scandinavia-northeastern European Russia and two minor centers over the central southern Mediterranean region and the Caucasus. Presumably, this mode might represent a lagged response to remote (like ENSO) signals. Local forcings (like heat fluxes from the Mediterranean and Black Seas) also may play a role. These possible links should be further investigated. In general, it is worth noting that our analysis did not reveal significant links between the ENSO and precipitation variability over Europe. Indeed, this result is not surprising. As was shown in some studies, precipitation in different European regions demonstrates significant links to ENSO during different seasons. For instance, *Mariotti et al.* [2002] investigated links between Euro-Mediterranean rainfall and ENSO and found spatially coherent correlation patterns in central and eastern Europe during winter and spring, and in western Europe and the Mediterranean region during fall and spring. Therefore, when the precipitation variability over the whole of Europe is analyzed, precipitation variations in some regions may mask ENSO-related precipitation variability in other European regions. Moreover, according to *Rodo et al.* [1997], the delay between the ENSO mature phase in winter (DJF) and its impact on precipitation over southern Europe ranges between 3 and 15 months. Thus our analysis, restricted to simultaneous connections between winter and summer precipitation fields over Europe and major teleconnection patterns, could not reveal significant links to ENSO.

[49] In the present study we described and analyzed the key features of seasonality in both interannual and intra-seasonal variability of precipitation over Europe. Basically, prominent seasonal differences were detected in all considered parameters, describing precipitation variability over Europe (i.e., climatologies, SDs, leading EOF modes). Since the large portion of Europe receives essentially a larger amount of precipitation during the summer season (compared with the winter season), the importance of further detailed analysis of its variability is evident. Particularly because we failed to reveal statistically significant modes of summer intraseasonal precipitation fluctuations, further study in this direction based on analysis of daily precipitation time series (with possible separation into different synoptic timescales) would be of great interest. Both diagnostic studies of the observational data and model experiments can provide useful information for the summer climate prediction. Thus present results imply that more attention should be paid to further analysis of summertime climate variability in the region.

[50] **Acknowledgments.** This research was supported by the Russian Foundation for Basic Research grant 01-05-64174. The CRU05 data have been supplied by the Climate Impacts LINK Project (UK Department of the Environment contract EPG 1/1/16) on behalf of the Climatic Research Unit, University of East Anglia. The author thanks Patrick Market and Richard Allan for their reading and careful editing of the manuscript. Discussions with Sergey Gulev as well as his useful comments are greatly appreciated. The author thanks Julia Zulyaeva for assistance in some calculations. The manuscript was improved by the constructive comments of anonymous reviewers.

References

- Appenzeller, C., J. Schwander, S. Sommer, and T. F. Stocker (1998), The North Atlantic Oscillation and its imprint on precipitation and ice accumulation in Greenland, *Geophys. Res. Lett.*, 25, 1939–1942.
- Barnston, A. G., and R. E. Livezey (1987), Classification, seasonality and persistence of low-frequency atmospheric circulation patterns, *Mon. Weather Rev.*, 115, 1083–1126.
- Bendat, J. S., and A. G. Piersol (1966), *Measurement and Analysis of Random Data*, 390 pp., John Wiley, Hoboken, N. J.
- Beniston, M. (1997), Variations of snow depth and duration in the Swiss Alps over the last 50 years: Links to changes in large-scale climatic forcings, *Clim. Change*, 36, 281–300.
- Blasing, T. J. (1979), Map pattern classification at a prescribed level of generality, in *Sixth Conference on Probability and Statistics in the Atmospheric Sciences*, pp. 118–125, Am. Meteorol. Soc., Boston, Mass.
- Blasing, T. J. (1981), Characteristic anomaly patterns of summer sea level pressure for the Northern Hemisphere, *Tellus*, 33, 428–437.
- Bradley, R. S., H. F. Diaz, J. K. Eischeid, P. D. Jones, P. M. Kelly, and C. M. Goodess (1987), Precipitation fluctuation over Northern Hemisphere land areas since the mid-19th century, *Science*, 237, 171–175.
- Cassou, C., and L. Terray (2001), Oceanic forcing of the wintertime low-frequency atmospheric variability in the North Atlantic-European sector: A study with the APREGE model, *J. Clim.*, 14, 4266–4291.
- Chu, P.-S., and R. W. Katz (1989), Spectral estimation from time series models with relevance to the Southern Oscillation, *J. Clim.*, 2, 86–90.
- Colman, A., and M. Davey (1999), Prediction of summer temperature, rainfall and pressure in Europe from preceding winter North Atlantic ocean temperature, *Int. J. Climatol.*, 19, 513–536.
- Corte-Real, J., B. Qian, and H. Xu (1998), Regional climate change in Portugal: Precipitation variability associated with large-scale atmospheric circulation, *Int. J. Climatol.*, 18, 619–635.
- Dai, A., and T. M. L. Wigley (2000), Global patterns of ENSO-induced precipitation, *Geophys. Res. Lett.*, 27, 1283–1286.
- Dai, A., I. Y. Fung, and A. D. Del Genio (1997), Surface observed global land precipitation variations 1900–88, *J. Clim.*, 10, 2943–2962.
- Diaz, H. F., R. S. Bradley, and J. K. Eischeid (1989), Precipitation fluctuation over global land areas since the late 1800s, *J. Geophys. Res.*, 94, 1195–1210.
- Dirmeyer, P. A., M. J. Fennessy, and L. Marx (2003), Low skill in dynamical prediction of boreal summer climate: Grounds for looking beyond sea surface temperature, *J. Clim.*, 16, 995–1002.
- Drevillon, M., L. Terray, P. Rogel, and C. Cassou (2001), Mid latitude Atlantic SST influence on European climate variability in the NCEP reanalysis, *Clim. Dyn.*, 18, doi:10.1007/s003820100178.
- Fraedrich, K., and K. Muller (1992), Climate anomalies in Europe associated with ENSO extremes, *Int. J. Climatol.*, 12, 25–31.
- Hurrell, J. W. (1995), Decadal trends in the North Atlantic Oscillation: Regional temperature and precipitation, *Science*, 269, 676–679.
- Hurrell, J. W., and C. K. Folland (2002), A change in the summer atmospheric circulation over the North Atlantic, *CLIVAR Exch.*, 7(3–4), 52–54.
- Johansson, A., A. Barnston, S. Saha, and H. Van den Dool (1998), On the level and origin of seasonal forecast skill in Europe, *J. Atmos. Sci.*, 55, 103–127.
- Kalnay, E., et al. (1996), The NCEP/NCAR 40-year reanalysis project, *Bull. Am. Meteorol. Soc.*, 77(3), 437–471.
- Korzun, V. I., A. A. Sokolov, M. I. Budyko, K. P. Voskresensky, G. P. Kalinin, A. A. Konoplyaqtsev, E. S. Korotkevich, and M. I. L'vovitch (Eds.) (1978), *Atlas of World Water Balance*, 663 pp., USSR Natl. Comm. for the Int. Hydrol. Decade, U. N. Educ., Sci. and Cult. Organ., Paris.
- Legates, D. R. (1987), A climatology of global precipitation, *Publ. Climatol.*, 40(1), 85 pp.
- Legates, D. R., and C. J. Willmott (1990), Mean seasonal and spatial variability in gauge-corrected, global precipitation, *Int. J. Climatol.*, 10, 111–127.
- Mariotti, A., N. Zeng, and K.-M. Lau (2002), Euro-Mediterranean rainfall and ENSO: A seasonally varying relationship, *Geophys. Res. Lett.*, 29(12), 1621, doi:10.1029/2001GL014248.
- Nakamura, H. (1996), Year-to-year and interdecadal variability in the activity of intraseasonal fluctuations in the Northern Hemisphere wintertime circulation, *Theor. Appl. Climatol.*, 55, 19–32.
- New, M. G., M. Hulme, and P. D. Jones (1999), Representing twentieth-century space-time climate variability: I. Development of 1961–90 mean monthly terrestrial climatology, *J. Clim.*, 12, 829–856.
- New, M. G., M. Hulme, and P. D. Jones (2001), Representing twentieth-century space-time climate variability: II. Development of a 1901–96 monthly grids of terrestrial surface climate, *J. Clim.*, 13, 2217–2238.
- North, G. R., T. L. Bell, and R. F. Calahan (1982), Sampling errors in the estimation of empirical orthogonal functions, *Mon. Weather Rev.*, 110, 699–706.

- Portis, D. H., J. E. Walsh, M. El Hamly, and P. J. Lamb (2001), Seasonality of the North Atlantic Oscillation, *J. Clim.*, **14**, 2069–2078.
- Qian, B., H. Xu, and J. Corte-Real (2000), Spatial-temporal structures of quasi-periodic oscillations in precipitation over Europe, *Int. J. Climatol.*, **20**, 1583–1598.
- Rodo, X., E. Baert, and F. A. Comin (1997), Variations in seasonal rainfall in southern Europe during the present century: Relationships with the North Atlantic Oscillation and the El Niño Southern Oscillation, *Clim. Dyn.*, **13**, 275–284.
- Rodwell, M. J., D. P. Rowell, and C. K. Folland (1999), Oceanic forcing of the wintertime North Atlantic Oscillation and European climate, *Nature*, **398**, 320–323.
- Rogers, J. C. (1990), Patterns of low-frequency monthly sea level pressure variability (1899–1986) and associated wave cyclone frequencies, *J. Clim.*, **3**, 1364–1379.
- Rogers, J. C. (1997), North Atlantic storm track variability and its association to the North Atlantic Oscillation and climate variability of northern Europe, *J. Clim.*, **10**, 1635–1647.
- Ropelewski, C. F., and P. D. Jones (1987), An extension of the Tahiti–Darwin Southern Oscillation Index, *Mon. Weather Rev.*, **115**, 2161–2165.
- Shabalova, M. V., and S. L. Weber (1998), Seasonality of low-frequency variability in early-instrumental European temperatures, *Geophys. Res. Lett.*, **25**, 3859–3862.
- Slonosky, V. C., P. D. Jones, and T. D. Davies (2001), Atmospheric circulation and surface temperature in Europe from the 18th century to 1995, *Int. J. Climatol.*, **21**, 63–75.
- Trenberth, K. E. (1999), Atmospheric moisture recycling: Role of advection and local evaporation, *J. Clim.*, **12**, 1368–1381.
- Trenberth, K. E., G. W. Branstator, D. Karoly, A. Kumar, N.-C. Lau, and C. Ropelewski (1998), Progress during TOGA in understanding and modeling global teleconnections associated with tropical sea surface temperatures, *J. Geophys. Res.*, **103**, 14,291–14,324.
- Trenberth, K. E., A. Dai, R. M. Rasmusson, and D. B. Parsons (2003), The changing character of precipitation, *Bull. Am. Meteorol. Soc.*, **84**, 1205–1217.
- von Storch, H., and A. Navarra (1995), *Analysis of Climate Variability*, 334 pp., Springer-Verlag, New York.
- von Storch, H., E. Zorita, and U. Cubasch (1993), Downscaling of global climate change estimates to regional scales: An application to Iberian rainfall in wintertime, *J. Clim.*, **6**, 1161–1171.
- Wibig, J. (1999), Precipitation in Europe in relation to circulation patterns at the 500 hPa level, *Int. J. Climatol.*, **19**, 253–269.
- Wilks, D. S. (1995), *Statistical Methods in the Atmospheric Sciences*, 467 pp., Academic, San Diego, Calif.
- Xie, P., and P. Arkin (1996), Analyses of global monthly precipitation using gauge observations, satellite estimates, and numerical model predictions, *J. Clim.*, **9**, 840–858.
- Xie, P., and P. Arkin (1997), Global precipitation: A 17-year monthly analysis based on gauge observations, satellite estimates, and numerical model outputs, *Bull. Am. Meteorol. Soc.*, **78**, 2539–2558.
- Zorita, E., V. Kharin, and H. von Storch (1992), The atmospheric circulation and sea surface temperature in the North Atlantic area in winter: Their interaction and relevance for Iberian precipitation, *J. Clim.*, **5**, 1097–1108.
- Zvereva, I. I. (1999), Decadal and longer changes of the winter sea level pressure fields and related synoptic activity over the North Atlantic, *Int. J. Climatol.*, **19**, 1177–1185.

I. I. Zvereva, P. P. Shirshov Institute of Oceanology, RAS 36, Nakhimovsky Avenue, Moscow, 117851, Russia. (igorz@sail.msk.ru)